HHS Public Access

Author manuscript

Abdom Imaging. Author manuscript; available in PMC 2016 February 03.

Published in final edited form as:

Abdom Imaging. 2015 April ; 40(4): 766–775. doi:10.1007/s00261-015-0347-6.

Non-invasive detection of liver fibrosis: MR imaging features vs. MR elastography

Sudhakar K. Venkatesh, M.D.[1], **Meng Yin, Ph.D.**[1], **Naoki Takahashi, M.D.**[1], **James F. Glockner, M.D.**[1], **Jayant A. Talwalkar, M.D.**[2], and **Richard L. Ehman, M.D.**[1]

[1]Department of Radiology, Mayo Clinic College of Medicine, Rochester, MN

[2]Department of Gastroenterology and Hepatology, Mayo Clinic College of Medicine, Rochester, MN

Abstract

Purpose—To compare accuracy of morphological features of liver on MRI and liver stiffness with MR elastography (MRE) for detection of significant liver fibrosis and cirrhosis.

Materials and Methods—In this retrospective study, we evaluated 62 patients who underwent liver MRI with MRE and histological confirmation of liver fibrosis within 6 months. Two radiologists, blinded to histology results, independently evaluated liver parenchyma texture, surface nodularity, signs of volumetric changes and portal hypertension for presence of significant fibrosis and cirrhosis. Two more readers independently calculated mean liver stiffness values with MRE. Interobserver agreement was evaluated with kappa and intra-class correlation coefficient (ICC) analysis. Diagnostic accuracy was assessed with area under receiver operating characteristic (AUROC) analysis. Comparison of AUROCs of MRI and MRE was performed.

Results—Liver fibrosis was present in 37 patients. The interobserver agreement was poor to good (kappa= 0.12 - 0.74) for MRI features and excellent for MRE (ICC, 0.97, 95% CI, 0.95-0.98). MRI features had 48.5-87.9%sensitivity, 55.2%-100%specificity and 71.5-81.6% accuracy //for detection of significant fibrosis. MRE performed better with 100% sensitivity, 96.5% specificity and 98.9% accuracy .For the detection of cirrhosis, MRE performed better than MRI features with 88.2% sensitivity (vs.41.2-82.3%), 91.1% specificity (vs. 64.4-95.6%) and 93.5% accuracy (vs. 60.6%-80.5%) Among the MRI features, surface nodularity and overall impression had the best accuracies of 80.3% and 81.6% for detection of significant fibrosis respectively. For cirrhosis, parenchyma texture and overall impression had the best accuracies of 80.5% and 79.7% respectively . Overall, MRE had significantly greater AUROC than MRI features for detection of both significant fibrosis (0.98.9 vs 0.71-0.82, $p<0.001$) and cirrhosis (0.93.5-vs. 0.61 -0.80.5, $p<0.01$).

Conclusion—MRE is superior to MRI for the non-invasive diagnosis of significant liver fibrosis and cirrhosis.

Address correspondence to: Sudhakar Kundapur Venkatesh, MD, vekatesh.sudhakar@mayo.edu, 200 1st St SW, Rochester, MN 55905, USA.

Institutions where work originated: Mayo Clinic College of Medicine, Rochester, MN Address: 200 First St. SW, Rochester, MN 55905

Introduction

Chronic liver disease and cirrhosis remains a major public health problem worldwide with significant morbidity and mortality. In the United States, approximately 150,000 individuals are diagnosed with chronic liver disease annually with nearly 20% of them with advanced fibrosis or cirrhosis of the liver. Nearly 36,000 patients die every year from complications attributable to cirrhosis(1, 2) The total health care burden attributable to chronic liver disease is more than 1.5billion (1) The mortality rate in patients with cirrhosis increases to 57% once decompensation and liver failure develops (3). However, liver fibrosis is reversible with specific treatment of the underlying hepatic disease (4-7) in almost the entire spectrum of chronic liver diseases (8). The early detection of clinically significant liver fibrosis may facilitate a prompt intervention with specific therapies and risk factor modifications (9). Liver biopsy, the current gold standard for detecting liver fibrosis, is limited by reduced patient acceptance, sampling error and inter-observer variation with interpretation (10-13), and a small but important risk for morbidity (3%) (14). In contrast, safe, non-invasive markers of liver fibrosis would allow for repeated assessments to monitor disease progression or assess response to treatment while retaining similar accuracy as liver biopsy with improved patient acceptance.

Serum markers of liver fibrosis are attractive as they could be made widely available and used repeatedly for monitoring. However, an estimated 30-50% of individuals will still require a liver biopsy based on the intermediate results (15). In patients with chronic viral hepatitis, there is a poor correlation between symptoms or serum markers and the histologic stage of fibrosis or cirrhosis on liver biopsy (16).

Imaging techniques also provide a non-invasive way to predict liver fibrosis. Imaging features such as surface nodularity, heterogeneous parenchyma enhancement, small size of the liver due to atrophy of the right lobe, caudate lobe hypertrophy, splenomegaly, increased caudate to right lobe ratio (17, 18), varices, expanded gallbladder fossa sign (19), posterior hepatic notch sign (20) and ascites are well known to be associated with liver fibrosis and cirrhosis. Textural changes in liver parenchyma resulting from early or mild fibrosis may not be easily detected on conventional techniques. Imaging techniques, however, are useful in identifying features of advanced fibrosis and complications of liver cirrhosis such as portal hypertension and development of hepatocellular carcinoma (21). A number of MRI- based techniques have also been proposed for the detection of hepatic fibrosis. Dynamic contrast enhanced MRI of the liver can demonstrate signal intensity alterations in association with hepatic fibrosis, but these techniques are qualitative and may not be sufficiently sensitive to identify earlier stages of liver fibrosis (22-24). Dual contrast enhanced MRI techniques with gadolinium and iron oxide contrast agents does appear to enhance visualization of fibrosis (25), yet the ability to quantitatively assess the degree of hepatic fibrosis is lacking. Specialized quantitative MR techniques such as spectroscopy (26), diffusion (27, 28) and perfusion (29) are still limited in clinical value based on lack of consensus regarding the utility or preferred implementation of these methods. Elastography techniques that measure stiffness of tissues have been found useful for evaluation of liver fibrosis. Elastography techniques that are clinically useful are either ultrasound based or MRI based. Ultrasound based techniques include transient elastography (TE)(30), shear wave elastography (SWE)

(31), acoustic radiation force impulse imaging (ARFI)(32) and several other emerging techniques(33) TE measures tissue elasticity with excellent reproducibility among trained operators and is based on the assumption that fibrosis results in increased stiffness of the liver parenchyma (3, 34). Its clinical utility in North America, however, remains to be determined as the probability for technical failure is greatly increased with the presence of obesity (35-37). MRI based MR Elastography (MRE) has been shown to be a promising technique for the detection of liver fibrosis (38-41). TE and MRE are the most commonly used elastography techniques for the assessment of liver fibrosis. While TE can detect moderate to severe fibrosis with high accuracy, individuals with mild to moderate degrees of liver fibrosis are detected more accurately by MRE. In addition, MRE can differentiate normal liver from inflammation (39, 41-44). The performance of MRE is not dependent on the scanner magnetic field strength (1.5 or 3T) and the stiffness measured is dependent on the frequency of mechanical vibration used(45). MRE available on most vendor platforms perform the technique at 60Hz which allows for comparison across institutions and scanners.

Although advanced techniques are now available in several institutes, in some institutes where advanced techniques are not available, suspicion and/or prediction of liver fibrosis is dependent on identifying features on conventional imaging as a non-invasive method. . The purpose of our study is to compare the diagnostic accuracies of MRE with conventional MRI features for the detection of liver fibrosis.

Materials and Methods

Subjects

This Health Insurance Portability and Accountability Act-complaint study was approved by the IRB of our institute and waived the requirement for informed consent for retrospective data analysis. **The MRE sequence was performed as a clinical application along with the routine conventional MRI study of the liver.** Patients gave informed consent as a routine procedure for all MRI studies. The study population consisted of consecutive patients who had undergone a liver MRI study with MRE and had histopathological confirmation of fibrosis as the reference standard.

Sixty-six patients who underwent MRI with MRE had histological confirmation of fibrosis. Two patients were excluded from the study due to severe breath holding and motion artifacts in the MRI images rendering the images not suitable for assessment. Two patients were excluded due to high iron content in the liver which resulted in low signal from the liver parenchyma. The final study group was comprised of 62 patients (31 men and 31 women, mean age ± SD, 54.6 years ± 11.8, range 22 to 76 years). The indications for MRI study of the liver were suspected liver fibrosis (n=43), evaluation of liver mass/masses (n=17) and abnormal liver enzyme levels (n=2). The cause of chronic liver disease in patients with suspected liver fibrosis were non-alcoholic fatty liver disease (NAFLD) in 16, hepatitis C in 13, primary sclerosing cholangitis in 3, hepatitis B in 2; alcoholic liver disease in 2, autoimmune hepatitis in 2, cryptogenic in 2, alpha-1-antitrypsin deficiency in 1, hemochromatosis in 1and primary biliary cirrhosis in 1. The liver masses evaluated were metastases in seven (neuroendocrine-3, colonic-2, pancreatic-1 and melanoma-1), hepatic adenoma in three, cholangiocarcinoma in three, focal nodular hyperplasia in two,

hemangioma in one, and hepatocellular carcinoma in one. MRI and MRE were performed within 6 months of obtaining liver histology by either biopsy or surgical resection.

MRI technique

MRI was performed on 1.5T clinical MR scanners (Signa, GE Healthcare, Waukesha, WI, USA) with a phased-array torso coil. The standard liver imaging protocol comprised of a coronal T2 weighted Single shot fast spin echo, axial T2 weighted fast spin echo, fast gradient In-phase and opposed-phase, axial T1 weighted liver acquisition with volumetric acceleration (LAVA) before and post contrast dynamic triple phase (arterial, portal venous and delayed) LAVA sequences were obtained. Gadodiamide (Omniscan, Amersham Health) 0.1mmol/kg or Gadobenate dimeglumine (Multihance, Bracco) 0.1mmol/kg was injected intravenously at a rate of 2-3ml/s using an automated injector (MedRad, Pittsburg, PA) and was followed by a 30mL saline flush. A 2ml test bolus was performed to determine the scan delay following contrast injection to optimize the arterial phase acquisition. All the sequences were performed with patient breath hold in end-inspiration except for the respiratory-triggered sequence. The scan parameters are presented in table.1.

MR Elastography (MRE)

MRE was performed at the end after the standard MRI protocol. A cylindrical passive driver (19cm × 1.5cm) was placed against the right chest wall overlying the liver with its center at the level of xiphisternum. The passive driver was held in place with an abdominal binder. A continuous acoustic vibration at 60Hz was transmitted from an active driver to the passive driver via a flexible vinyl tube, to produce propagating shear waves in the liver (41, 46). The passive driver was easily introduced between the patients' chest /abdominal wall and the phased array coil without any effect on image quality. The propagating shear waves were imaged with a modified phase-contrast, gradient echo sequence (MRE sequence) to image axial “wave” images sensitized along the through-plane motion direction. The sequence parameters were: TR/TE= 100/25.6ms; bandwidth= ±31.25 kHz; flip angle= 30, FOV= 32-42cm; matrix 256× 96; slice thickness 10mm; gap 5 mm. There was no special limitation on the field of view for the MRE sequence. Four MRE slices were obtained in each patient. The total acquisition time was split into 4 periods of suspended respiration of 16 seconds to obtain wave images at 4-phase offsets. In order to obtain a consistent position of the liver for each phase offset, patients were asked to hold their breath at the end of expiration. The slices were prescribed through the largest cross-section of the liver. The wave images were then automatically processed by the inversion algorithm installed in the scanner (47, 48) to yield quantitative images of tissue shear stiffness maps, in units of kilopascals.

Image Analysis

MRI—Two fellowship trained abdominal radiologists with 12 and 15 years of experience in interpreting MRI studies of liver (R1 and R2) and blinded to the clinical indications, MRE data and histology analyzed the MRI images for liver fibrosis or cirrhosis. The features evaluated were liver texture, surface nodularity, regenerative nodules, liver contour changes, and signs of portal hypertension. Normal liver parenchyma texture was defined as homogeneous fine texture and a fibrotic liver texture was defined as inhomogeneous, coarse

texture with or without visualization of fibrous septa. The texture of the liver parenchyma for presence of fibrosis was analyzed on a scale of 1-4 (1-fibrosis definitely absent; 2-fibrosis probably absent; 3-fibrosis probably present; 4-fibrosis definitely present) on pre-contrast T2-W and T1-W and post gadolinium enhanced T1-W images. Normal liver has a smooth contour and sharp edges. Nodular liver was identified as one with an irregular contour with blunt or rounded edges. Surface nodularity was graded on a 1-4 point scale (1-nodularity absent; 2-mild nodularity; 3-moderate nodularity; 4-severe nodularity). Regenerative nodules were identified as nodular regions of liver parenchyma surrounded by a complete or incomplete fibrous septa and isointense to liver parenchyma on both T1 and T2 weighted images with no arterial phase hypervascularity or washout in portal/delayed phases. Regenerative nodules were reported as either present or absent. Signs of liver contour changes representing early and later stages of cirrhosis: expanded gall bladder fossa (EGBF) sign (19) or posterior hepatic notch (PHN) sign (20), were also assessed. Regional volumetric changes such as enlarged (>10mm) perihilar portal space (PPS) (49), caudate-right lobe ratio (CRL) (>0.65 representing cirrhosis) (18) and modified caudate-right lobe ratio (mCRL) (>0.90 representing cirrhosis) (50) were measured by a third independent reader who was available for the two radiologists (R1 and R2) when reviewing the images. In addition, features of portal hypertension including splenomegaly (>12cm length), esophageal varices or intra-abdominal collaterals, and ascites were assessed and reported as present or absent. Splenomegaly was considered to be present with splenic length was ≥13cm(51) Esophageal varices were identified as discrete enhancing nodular lesions abutting the luminal surface of the esophageal wall or contacting/ protruding into luminal space (52, 53). Abdominal collaterals were identified as enhancing tortuous channels 3-5mm diameter and in perigastric, per splenic, para umbilical or retroperitoneal locations. Ascites was defined as free fluid in the abdomen or pelvis. Based on all the MRI findings, an overall qualitative grading for the presence of fibrosis and/or cirrhosis was done on a 1-7 scale (1-no fibrosis; 2-fibrosis probably absent; 3- fibrosis probably present; 4-fibrosis present; 5-early cirrhosis; 6-advanced cirrhosis; 7-progressive cirrhosis).

Parenchyma texture grade ≥3, surface nodularity grade ≥2 and overall impression grade ≥4 were considered to represent significant fibrosis. An overall impression grade ≥5 was considered to represent cirrhosis. EGBF, RPHN, PPS (>10mm), CRL (>0.65), mCRL (>0.9), and features of portal hypertension (splenomegaly, ascites, and abdominal varices) when present were considered to be predictive of cirrhosis.

MRE—Two additional readers- an abdominal radiologist and a research scientist (R3 and R4) with 7 and 8 years of experience in reading MRE images and elastograms respectively calculated the mean shear stiffness values of the livers independently and were blinded to histology, clinical information and morphological scoring. Mean shear stiffness of the liver was calculated using a manually specified region of interest (ROI). The ROIs were drawn manually in the largest possible area of liver parenchyma which was illuminated with shear waves and excluded major blood vessels seen on the magnitude image obtained with the MRE sequence. ROIs were placed in individual slices and in the right lobe whenever possible, and the average value calculated from all slices was reported as mean stiffness in kilopascals. In patients with liver tumors, every attempt was made to obtain the values in the

image which showed the non-tumor bearing liver parenchyma most and preferably the slice which did not show any tumor. Stiffness was obtained from the other liver lobe when a larger tumor was present.

Comparing MRI with MRE

The MRI readings and MRE scores were converted into a single reading and score, respectively, to simplify comparison between MRI and MRE. The average of grades of the two readers R1 and R2 for parenchyma texture, regenerative nodules, surface nodularity and overall impression overall impression was used as MRI reading. The reading of EGBF, RPHN, and signs of portal hypertension (considered positive when at least one reader read as positive) combined into one single reading. The liver stiffness scores from readers R3 and R4 were averaged into one average MRE score. AUROCs of MRI and MRE for detection of significant fibrosis and cirrhosis were compared for significant differences.

Pathology

Histological evaluation of liver fibrosis was performed with percutaneous or transjugular liver biopsies in 54 patients and surgical resection in 8 patients. An institutional pathologist performed histological analysis and fibrosis staging per standard guidelines. Chronic liver disease was present in 43 patients and normal livers in 19 patients.

The stages of liver fibrosis were recorded. Significant fibrosis was defined as stage 2 fibrosis typically showing septa formation.

Statistical analysis

Inter-observer agreement for each morphological MRI features was evaluated with an inter rater agreement statistic with 95% confidence interval (K, kappa; <0.20- poor; 0.21-0.40 fair, 0.41-0.60 moderate, 0.61- 0.80 good and 0.81-1.00 very good). Interobserver agreement between MRE readers was assessed with intra class correlation analysis.

Receiver operating characteristic (ROC) analysis was performed for determining the optimal cut-off point of MRE stiffness (R3 and R4) for detection of significant fibrosis and cirrhosis. ROC analysis was also performed for MRI features by R1 and R2. Sensitivity, specificity and accuracy and 95% confidence intervals (95%CI) were derived. For comparison of MRI with MRE, areas under ROC (AUROC) were compared (54) for any significant differences between MRI morphology features and MRE for detection of significant fibrosis (≥ stage 2) and cirrhosis (stage 4). P-values <0.05 were considered statistically significant. All statistical analyses were performed with MedCalc Statistical Software version 12.7.7 (MedCalc Software bvba, Ostend, Belgium).

Results

Histology confirmed liver fibrosis in 37 patients with stage 1 in 4 patients, stage 2 in 5, stage 3 in 11, and stage 4 in 17 patients.

MRI readers rated abnormal parenchyma in 55 (88.7%); surface nodularity in 28 (45.2%); regenerative nodules present in 17 (27.4%); EGBF sign in 16 (25.8%), RPHN sign in 14

(22.6%) and overall impression of significant fibrosis in 33 (53.2%) and cirrhosis in 17 (27.4%).PPS was present in 18 (29%), CRL was positive in 16 (25.8%) and mCRL was positive in 26 (42%). Varices and/or abdominal collaterals were present in 22 (35.4%), splenomegaly in 25 (40.3%) and ascites in 15 (24.2%) The mean (±SD) liver stiffness with MRE was 4.5kPa (±2.4kPa) and ranged from1.8 to 11.4kPa.

Interobserver agreement

MRI features—The inter observer agreement for MRI features (Table2) was good for surface nodularity, ascites, splenomegaly and varices; moderate for regenerative nodules and overall impression; and fair for parenchyma texture and right posterior hepatic notch sign. There was poor interobserver agreement for expanded gall bladder fossa sign.

MRE—The intra class coefficient analysis showed an excellent agreement of 0.97 (95% CI, 0.95-0.98) for measured liver stiffness values between readers R3 and R4. The mean liver stiffness value for the entire cohort measured by R3 and R4 were 4.47kPa (95% CI, 3.87 -5.07) and 4.33kPa (95% CI, 3.75 – 4.9) respectively.

Detection of significant fibrosis

The sensitivity, specificity and accuracy for detection of significant fibrosis with MRI features were poor to good and excellent for MRE (Table.3). The cut-off value for significant fibrosis with MRE was 3.37kPa. AUROC of MRE (0.99) was significantly higher than parenchyma texture (vs.0.71, $p<0.0001$), regenerative nodules (vs.0.72, $p<0.0001$), surface nodularity (vs. 0.80, $p<0.0001$) and overall impression (vs.0.82, $P=0.0001$).

Detection of cirrhosis

The performance of MRI features was fair to good for detection of cirrhosis (Table.3). Parenchyma texture, regenerative nodules and surface nodularity had moderate to good accuracy. EGBF and RPHN had moderate accuracy with poor to fair sensitivity but good specificity for predicting cirrhosis. The signs of volumetric changes PPS, CRL and mCRL had fair sensitivities and moderate accuracies for predicting cirrhosis. Varices and splenomegaly had moderate to good sensitivity, specificity and accuracy for predicting cirrhosis. The presence of ascites was not a sensitive feature of cirrhosis but had excellent predictable specificity for cirrhosis. Overall impression had good sensitivity, specificity and accuracy for detection of cirrhosis. MRE had good sensitivity and excellent specificity and accuracy for predicting cirrhosis. The cut-off value for detecting cirrhosis was 5.2kPa.

Comparison of ROC curves showed that MRE performed (AUROC of 0.93) significantly better than parenchyma texture (vs. 0.80, $p= 0.02$) and nodularity (vs. 0.68, 0.0002). MRE had significantly higher diagnostic accuracy than EGBF (vs.60.6, $p<0.0001$) RPHN (vs. 0.67, $p=0.0003$), PPS (vs. 0.67, $p=0.0005$), CRL (vs.0.69, $p=0.0009$) and mCRL (vs.0.62, $p<0.0001$). MRE also performed significantly better than ascites (vs.0.70, $p<0.0003$), varices (vs. 0.74, $p=0.0018$) and splenomegaly (vs.0.79, $p=0.02$). Although overall impression had good performance, it was significantly inferior to MRE (vs.0.80, $p=0.019$).

Discussion

Our study results demonstrate that hat MRE is a better test for detection of significant liver fibrosis. Our study also confirms that MRE is superior to morphological features detected on MRI for the diagnosis of cirrhosis The performance of MRE was significantly better than each evaluated MRI feature and/or sign as well as the overall impression by two experienced abdominal radiologists. The interobserver agreement for MRE was excellent to almost perfect, whereas there was poor to moderate agreement between readers for MRI features. The higher performance of the MRE in our study is consistent with high accuracy reported in the literature (41, 43, 55-59) and has excellent performance for detection of fibrosis in study groups with multiple etiologies as well as those with single etiologies.

Clinically significant fibrosis defined as stage 2 fibrosis and above is an indication for treatment of chronic liver fibrosis (16). MRI features were not sufficiently accurate for detection of significant fibrosis in our study. Furthermore, the interobserver agreement for MRI features was fair to moderate. In our study, surface nodularity had the best interobserver agreement and was also the most accurate MRI feature for detection of significant fibrosis. Other features had fair to moderate accuracies and performed significantly inferior to MRE. MRE had an excellent accuracy for significant fibrosis. MRE measures liver stiffness that correlates with degree of fibrosis (60) and therefore be able to differentiate from normal liver as well as differentiate significant fibrosis from minimal fibrosis (41, 43, 59). Therefore, the utility of MRI features alone for detection of significant liver fibrosis is limited and MRE could replace conventional MRI because morphological features are less robust in detection of significant fibrosis and cirrhosis. especially when there are no volumetric changes which would increase a reader's suspicion for liver fibrosis.

MRI features had better specificity for detection of cirrhosis but accuracy was still moderate to good. The signs of volumetric changes, EGBF and RPHN had lower sensitivity and accuracy for detection of cirrhosis. Previous studies demonstrated a high degree of accuracy of 0.8 for both these signs (19, 20), but a study by Rustogi et al (61) showed accuracies between 0.54 - 0.66, similar to our results. The interobserver agreement for EGBF and RPHN was 0.12 and 0.45 in our study as compared to 0.44 and 0.53 in the study by Rustogi et al. These differences are probably related to different study populations and variable experience of the observers.

The volumetric signs of enlarged PPS, CRL and mCRL showed moderate accuracy for detection of cirrhosis. Enlarged PPS was reported as a helpful sign at MRI imaging in the diagnosis of cirrhosis (49) with an accuracy of 0.92, but in our study the accuracy was only 0.67. CRL and mCRL had moderate accuracy of 0.69 and 0.62 comparable to a wide range of accuracy of 0.57-0.94 (18, 61, 62) and 0.57-0.74 (50, 61) respectively, in the literature. The variable accuracies of these signs of volumetric changes make them unreliable for diagnosis of cirrhosis in routine clinical practice.

Varices and splenomegaly had higher specificity and accuracies compared to other MRI morphological signs. Ascites had high specificity but had low sensitivity and accuracy for detection of fibrosis. These results are not surprising as varices, splenomegaly and ascites

usually manifest in advanced cirrhosis and are uncommonly found in early fibrosis. Therefore signs of portal hypertension and ascites are most useful when present, and absence does not rule out cirrhosis.

Our study results are similar to Rustogi et al (61) who compared MRE with MRI for detection of severe fibrosis and cirrhosis. The performance of MRE in our study was better probably because we did not include any patient who received previous antiviral treatment and we included only patients with a biopsy performed within 6 months as compared to up to one year in the study by Rustogi et al. Antiviral treatment is known to cause reversal of fibrosis and may reduce fibrosis content. Longer duration between MRE and biopsy may result in progression of fibrosis especially in untreated patients. In our study we used a larger geographic ROI drawn over the liver as compared to three round/oval shaped ROIs in the study by Rustogi et al. Drawing larger ROI samples larger region of liver and this may resulted in better accuracy of MRE in our study. However, a future study comparing different regions of interest would be useful. Interestingly, however, there were no significant differences in the accuracy of MRI features in both studies.

Our study has limitations. The study population consisted of only 37 subjects as we had strict criteria of histologically confirmed liver fibrosis within 6 months of the MRE study to prevent progression of fibrosis bias. Due to the increasing availability of non-invasive tests including MRE, it is difficult to enroll patients with histological confirmation of liver fibrosis. Second, our study population also included a smaller number of patients with mild degree of fibrosis. This was unavoidable as patients with mild fibrosis usually do not manifest clinical symptoms or have abnormal liver function tests to warrant a liver biopsy. However our study results suggest that MRE is superior to MRI for detection of significant fibrosis. Third, our study population was heterogeneous in terms of etiology of chronic liver disease. Although, there is a possibility that the etiologies might affect the study results, our study focused on the final common endpoint of the disease, which is hepatic fibrosis. Presence of inflammation may affect the accuracy of MRE, especially in the lower stages of fibrosis (63, 64).Future studies on the influence of inflammation on MRI features may be useful. Fourth, we did not assess the influence of inflammation on MRE or on the MRI features. In our study population, there were no cases of acute flare up of the chronic viral hepatitis, and there were no laboratory findings or clinical suspicion of acute hepatic inflammation. Thus, the influence of acute hepatic inflammation on liver stiffness would be minimal. While some studies have shown that inflammatory activity might increase the stiffness values evaluated with TE, other studies with MRE have not shown such influence (56, 59). Commonly used MRE technique is gradient echo based phase contrast technique which sensitive to presence of paramagnetic substances such as iron. Therefore, in the case of severe iron overload, MRE may fail due to low signal from liver parenchyma. In these situations, TE and other ultrasound based technique maybe useful for assessment of liver fibrosis. Another MRI based technique that assess liver strain with tagging technique has been shown to be useful in differentiating cirrhotic livers from normal liver(65), however, its utility in mild fibrosis is not well established. Finally our study population comprised of patients with liver tumors. It is possible that large tumors may cause increased local stiffness on the surrounding liver parenchyma and therefore affect liver stiffness evaluation with MRE. However in our experience we did not observe significant change in liver stiffness in

entire liver parenchyma. Single tumor was present in all patients with tumors except one with multiple metastases. There was a sufficiently large region of parenchyma away from liver tumor for evaluation and specifically we used the other lobe unaffected by the tumor. Future studies are needed to systematically evaluate the effect of liver tumor on parenchymal stiffness evaluation.

In conclusion MR Elastography is more accurate than MRI features for detection of significant liver fibrosis and cirrhosis. Evaluation of liver for fibrosis with MRE may be particularly useful when MRI features of fibrosis and cirrhosis are absent.

References

1. Everhart JE, Ruhl CE. Burden of digestive diseases in the United States Part III: Liver, biliary tract, and pancreas. Gastroenterology. 2009; 136(4):1134–44. [PubMed: 19245868]
2. Asrani SK, Larson JJ, Yawn B, Therneau TM, Kim WR. Underestimation of liver-related mortality in the United States. Gastroenterology. 2013; 145(2):375–82. e1–2. [PubMed: 23583430]
3. de Franchis R, Dell'Era A. Non-invasive diagnosis of cirrhosis and the natural history of its complications. Best practice & research. 2007; 21(1):3–18. [PubMed: 17223493]
4. Bataller R, Brenner DA. Liver fibrosis. The Journal of clinical investigation. 2005; 115(2):209–18. [PubMed: 15690074]
5. Friedman SL. Liver fibrosis -- from bench to bedside. Journal of hepatology. 2003; 38(Suppl 1):S38–53. [PubMed: 12591185]
6. Rockey DC. Antifibrotic therapy in chronic liver disease. Clin Gastroenterol Hepatol. 2005; 3(2): 95–107. [PubMed: 15704042]
7. Rockey DC, Bissell DM. Noninvasive measures of liver fibrosis. Hepatology. 2006; 43(2 Suppl 1):S113–20. [PubMed: 16447288]
8. Friedman SL, Bansal MB. Reversal of hepatic fibrosis -- fact or fantasy? Hepatology. 2006; 43(2 Suppl 1):S82–8. [PubMed: 16447275]
9. Zhang Y, Zhang XM, Prowda JC, et al. Changes in hepatic venous morphology with cirrhosis on MRI. J Magn Reson Imaging. 2009; 29(5):1085–92. [PubMed: 19388123]
10. Bravo AA, Sheth SG, Chopra S. Liver biopsy. The New England journal of medicine. 2001; 344(7):495–500. [PubMed: 11172192]
11. Ratziu V, Charlotte F, Heurtier A, et al. Sampling variability of liver biopsy in nonalcoholic fatty liver disease. Gastroenterology. 2005; 128(7):1898–906. [PubMed: 15940625]
12. Standish RA, Cholongitas E, Dhillon A, Burroughs AK, Dhillon AP. An appraisal of the histopathological assessment of liver fibrosis. Gut. 2006; 55(4):569–78. [PubMed: 16531536]
13. Bedossa P, Dargere D, Paradis V. Sampling variability of liver fibrosis in chronic hepatitis C. Hepatology. 2003; 38(6):1449–57. [PubMed: 14647056]
14. Piccinino F, Sagnelli E, Pasquale G, Giusti G. Complications following percutaneous liver biopsy. A multicentre retrospective study on 68,276 biopsies. J Hepatology. 1986; 2(2):165–73.
15. Parkes J, Guha IN, Roderick P, Rosenberg W. Performance of serum marker panels for liver fibrosis in chronic hepatitis C. J Hepatology. 2006; 44(3):462–74.
16. Castera L. Noninvasive methods to assess liver disease in patients with hepatitis B or C. Gastroenterology. 2012; 142(6):1293–302. e4. [PubMed: 22537436]
17. Ito K, Mitchell DG. Hepatic morphologic changes in cirrhosis: MR imaging findings. Abdominal imaging. 2000; 25(5):456–61. [PubMed: 10931978]
18. Harbin WP, Robert NJ, Ferrucci JT Jr. Diagnosis of cirrhosis based on regional changes in hepatic morphology: a radiological and pathological analysis. Radiology. 1980; 135(2):273–83. [PubMed: 7367613]
19. Ito K, Mitchell DG, Gabata T, Hussain SM. Expanded gallbladder fossa: simple MR imaging sign of cirrhosis. Radiology. 1999; 211(3):723–6. [PubMed: 10352597]

20. Ito K, Mitchell DG, Kim MJ, Awaya H, Koike S, Matsunaga N. Right posterior hepatic notch sign: a simple diagnostic MR finding of cirrhosis. J Magn Reson Imaging. 2003; 18(5):561–6. [PubMed: 14579399]
21. Gaiani S, Gramantieri L, Venturoli N, et al. What is the criterion for differentiating chronic hepatitis from compensated cirrhosis? A prospective study comparing ultrasonography and percutaneous liver biopsy. Journal of hepatology. 1997; 27(6):979–85. [PubMed: 9453422]
22. Aube C, Racineux PX, Lebigot J, et al. Diagnosis and quantification of hepatic fibrosis with diffusion weighted MR imaging: preliminary results. Journal de radiologie. 2004; 85(3):301–6. [PubMed: 15192522]
23. Chen JH, Chai JW, Shen WC. Magnetization transfer contrast imaging of liver cirrhosis. Hepato-gastroenterology. 1999; 46(29):2872–7. [PubMed: 10576364]
24. Yeh WC, Li PC, Jeng YM, et al. Elastic modulus measurements of human liver and correlation with pathology. Ultrasound in medicine & biology. 2002; 28(4):467–74. [PubMed: 12049960]
25. Aguirre DA, Behling CA, Alpert E, Hassanein TI, Sirlin CB. Liver fibrosis: noninvasive diagnosis with double contrast material-enhanced MR imaging. Radiology. 2006; 239(2):425–37. [PubMed: 16641352]
26. Cho SG, Kim MY, Kim HJ, et al. Chronic hepatitis: in vivo proton MR spectroscopic evaluation of the liver and correlation with histopathologic findings. Radiology. 2001; 221(3):740–6. [PubMed: 11719670]
27. Koinuma M, Ohashi I, Hanafusa K, Shibuya H. Apparent diffusion coefficient measurements with diffusion-weighted magnetic resonance imaging for evaluation of hepatic fibrosis. J Magn Reson Imaging. 2005; 22(1):80–5. [PubMed: 15971188]
28. Taouli B, Losada M, Holland A, Krinsky G. Magnetic resonance imaging of hepatocellular carcinoma. Gastroenterology. 2004; 127(5 Suppl 1):S144–52. [PubMed: 15508078]
29. Pandharipande PV, Krinsky GA, Rusinek H, Lee VS. Perfusion imaging of the liver: current challenges and future goals. Radiology. 2005; 234(3):661–73. [PubMed: 15734925]
30. Sandrin L, Fourquet B, Hasquenoph JM, et al. Transient elastography: a new noninvasive method for assessment of hepatic fibrosis. Ultrasound in medicine & biology. 2003; 29(12):1705–13. [PubMed: 14698338]
31. Sarvazyan AP, Rudenko OV, Swanson SD, Fowlkes JB, Emelianov SY. Shear wave elasticity imaging: a new ultrasonic technology of medical diagnostics. Ultrasound Med Biol. 1998; 24(9): 1419–35. [PubMed: 10385964]
32. Nightingale K, Soo MS, Nightingale R, Trahey G. Acoustic radiation force impulse imaging: in vivo demonstration of clinical feasibility. Ultrasound Med Biol. 2002; 28(2):227–35. [PubMed: 11937286]
33. Sarvazyan A, Hall TJ, Urban MW, Fatemi M, Aglyamov SR, Garra BS. An overview of elastography - an emerging branch of medical imaging. Curr Med Imaging Rev. 2011; 7(4):255–82. [PubMed: 22308105]
34. Sandrin L, Fourquet B, Hasquenoph JM, et al. Transient elastography: a new noninvasive method for assessment of hepatic fibrosis. Ultrasound in medicine & biology. 2003; 29(12):1705–13. [PubMed: 14698338]
35. Castera L, Vergniol J, Foucher J, et al. Prospective comparison of transient elastography, Fibrotest, APRI, and liver biopsy for the assessment of fibrosis in chronic hepatitis C. Gastroenterology. 2005; 128(2):343–50. [PubMed: 15685546]
36. Foucher J, Castera L, Bernard PH, et al. Prevalence and factors associated with failure of liver stiffness measurement using FibroScan in a prospective study of 2114 examinations. European journal of gastroenterology & hepatology. 2006; 18(4):411–2. [PubMed: 16538113]
37. Ziol M, Handra-Luca A, Kettaneh A, et al. Noninvasive assessment of liver fibrosis by measurement of stiffness in patients with chronic hepatitis C. Hepatology. 2005; 41(1):48–54. [PubMed: 15690481]
38. Huwart L, Peeters F, Sinkus R, et al. Liver fibrosis: non-invasive assessment with MR elastography. NMR in biomedicine. 2006; 19(2):173–9. [PubMed: 16521091]

39. Huwart L, Sempoux C, Salameh N, et al. Liver fibrosis: noninvasive assessment with MR elastography versus aspartate aminotransferase-to-platelet ratio index. Radiology. 2007; 245(2): 458–66. [PubMed: 17940304]
40. Rouviere O, Yin M, Dresner MA, et al. MR elastography of the liver: preliminary results. Radiology. 2006; 240(2):440–8. [PubMed: 16864671]
41. Yin M, Talwalkar JA, Glaser KJ, et al. Assessment of hepatic fibrosis with magnetic resonance elastography. Clin Gastroenterol Hepatol. 2014; 5(10):1207–13. e2. 2007. [PubMed: 17916548]
42. Venkatesh SK, Ehman RL. Magnetic Resonance Elastography of Liver. Magn Reson Imaging Clin N Am. 22(3):433–46. [PubMed: 25086938]
43. Ichikawa S, Motosugi U, Ichikawa T, et al. Magnetic resonance elastography for staging liver fibrosis in chronic hepatitis C. Magn Reson Med Sci. 2012; 11(4):291–7. [PubMed: 23269016]
44. Chen J, Talwalkar JA, Yin M, Glaser KJ, Sanderson SO, Ehman RL. Early Detection of Nonalcoholic Steatohepatitis in Patients with Nonalcoholic Fatty Liver Disease by Using MR Elastography. Radiology. 2011; 259(3):749–56. [PubMed: 21460032]
45. Venkatesh SK, Ehman RL. Magnetic resonance elastography of liver. Magn Reson Imaging Clin N Am. 2014; 22(3):433–46. [PubMed: 25086938]
46. Venkatesh SK, Yin M, Ehman RL. Magnetic resonance elastography of liver: technique, analysis, and clinical applications. J Magn Reson Imaging. 2013; 37(3):544–55. [PubMed: 23423795]
47. Manduca A, Oliphant TE, Dresner MA, et al. Magnetic resonance elastography: non-invasive mapping of tissue elasticity. Medical image analysis. 2001; 5(4):237–54. [PubMed: 11731304]
48. Westin CF, Wigstrom L, Loock T, Sjoqvist L, Kikinis R, Knutsson H. Three-dimensional adaptive filtering in magnetic resonance angiography. J Magn Reson Imaging. 2001; 14(1):63–71. [PubMed: 11436216]
49. Ito K, Mitchell DG, Gabata T. Enlargement of hilar periportal space: a sign of early cirrhosis at MR imaging. J Magn Reson Imaging. 2000; 11(2):136–40. [PubMed: 10713945]
50. Awaya H, Mitchell DG, Kamishima T, Holland G, Ito K, Matsumoto T. Cirrhosis: modified caudate-right lobe ratio. Radiology. 2002; 224(3):769–74. [PubMed: 12202712]
51. Pozo AL, Godfrey EM, Bowles KM. Splenomegaly: investigation, diagnosis and management. Blood Rev. 2009; 23(3):105–11. [PubMed: 19062140]
52. Kim H, Choi D, Gwak GY, et al. Evaluation of esophageal varices on liver computed tomography: receiver operating characteristic analyses of the performance of radiologists and endoscopists. J Gastroenterol Hepatol. 2009; 24(9):1534–40. [PubMed: 19486446]
53. Lipp MJ, Broder A, Hudesman D, et al. Detection of esophageal varices using CT and MRI. Dig Dis Sci. 2011; 56(9):2696–700. [PubMed: 21380758]
54. DeLong ER, DeLong DM, Clarke-Pearson DL. Comparing the areas under two or more correlated receiver operating characteristic curves: a nonparametric approach. Biometrics. 1988; 44(3):837–45. [PubMed: 3203132]
55. Huwart L, Sempoux C, Vicaut E, et al. Magnetic resonance elastography for the noninvasive staging of liver fibrosis. Gastroenterology. 2008; 135(1):32–40. [PubMed: 18471441]
56. Huwart L, Salameh N, ter Beek L, et al. MR elastography of liver fibrosis: preliminary results comparing spin-echo and echo-planar imaging. Eur Radiol. 2008; 18(11):2535–41. [PubMed: 18504591]
57. Huwart L, Sempoux C, Salameh N, et al. Liver fibrosis: noninvasive assessment with MR elastography versus aspartate aminotransferase-to-platelet ratio index. Radiology. 2007; 245(2): 458–66. [PubMed: 17940304]
58. Huwart L, Peeters F, Sinkus R, et al. Liver fibrosis: non-invasive assessment with MR elastography. NMR Biomed. 2006; 19(2):173–9. [PubMed: 16521091]
59. Venkatesh SK, Wang G, Lim SG, Wee A. Magnetic resonance elastography for the detection and staging of **liver** fibrosis in chronic hepatitis B. Eur Radiol. 2014; 24(1):70–8. [PubMed: 23928932]
60. Venkatesh SK, Xu S, Tai D, Yu H, Wee A. Correlation of MR elastography with morphometric quantification of liver fibrosis (Fibro-C-Index) in chronic hepatitis B. Magn Reson Med. 2014; 72(4):1123–9. [PubMed: 24166665]

61. Rustogi R, Horowitz J, Harmath C, et al. Accuracy of MR elastography and anatomic MR imaging features in the diagnosis of severe hepatic fibrosis and cirrhosis. J Magn Reson Imaging. 2012; 35(6):1356–64. [PubMed: 22246952]

62. Giorgio A, Amoroso P, Lettieri G, et al. Cirrhosis: value of caudate to right lobe ratio in diagnosis with. US Radiology. 1986; 161(2):443–5. [PubMed: 3532188]

63. Shi Y, Guo Q, Xia F, et al. MR elastography for the assessment of hepatic fibrosis in patients with chronic hepatitis B infection: does histologic necroinflammation influence the measurement of hepatic stiffness? Radiology. 2014; 273(1):88–98. [PubMed: 24893048]

64. Ichikawa S, Motosugi U, Nakazawa T, et al. Hepatitis activity should be considered a confounder of liver stiffness measured with MR elastography. J Magn Reson Imaging. 2014 Epub ahead of print.

65. Chung S, Breton E, Mannelli L, Axel L. Liver stiffness assessment by tagged MRI of cardiac-induced liver motion. Magn Reson Med. 2011; 65(4):949–55. [PubMed: 21337420]

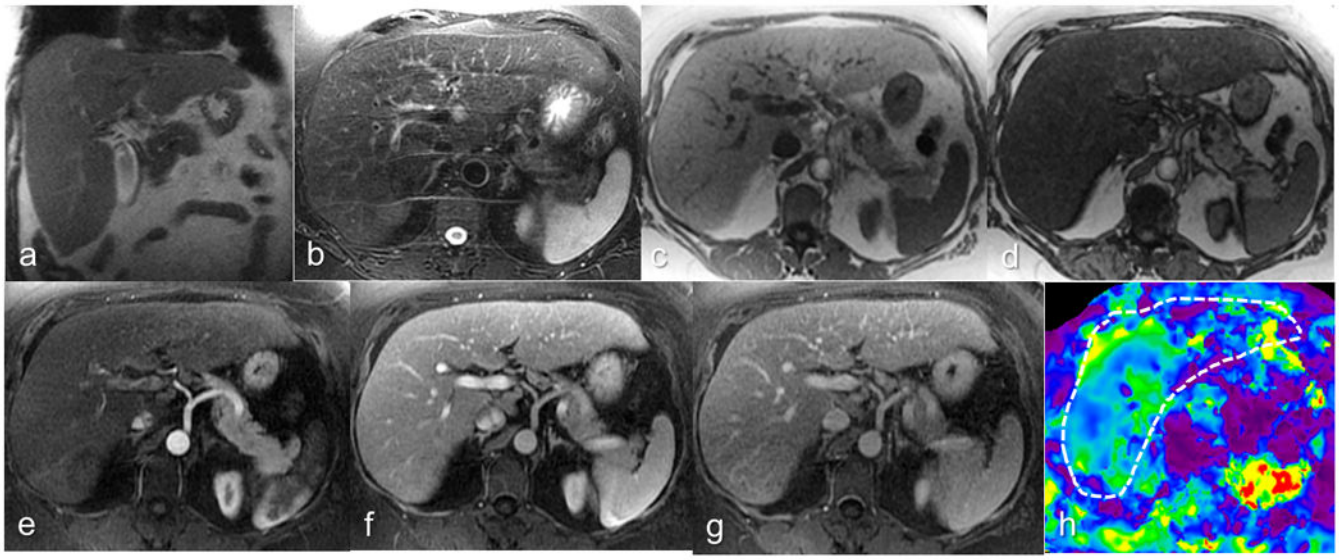

Figure 1.

Chronic hepatitis C patient with biopsy-confirmed stage 2 fibrosis. Coronal T2-W (a), axial T2-W (b), axial In (c) and opposed phase (d), post contrast arterial phase (e), portal venous phase (f) and delayed phase (g) images and elastogram (h) at the same level. R1 graded parenchyma texture-3 (fibrosis probably present), regenerative nodule-absent, surface nodularity-absent and overall impression-3 (fibrosis probably present). R2 graded parenchyma texture-1 (fibrosis absent), regenerative nodule-absent, surface nodularity-absent and overall impression-1 (no fibrosis) . Both readers' impression was significant liver fibrosis absent. The mean stiffness measured by the MRE readers R3 and R4 were 3.65 and 3.45kPa and both correctly classified the case as positive for significant fibrosis.

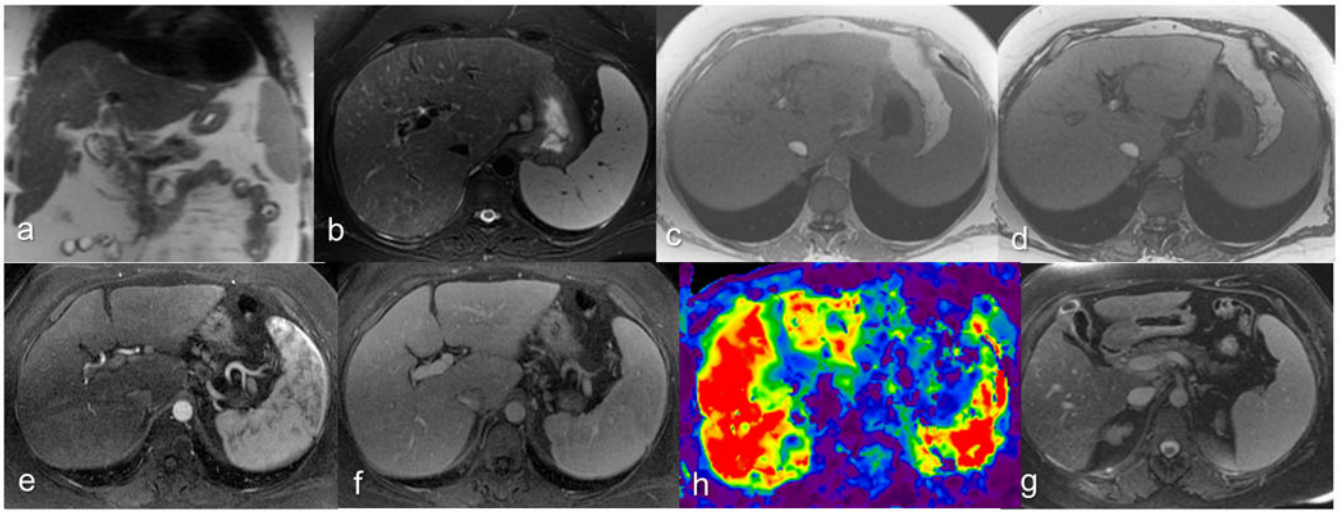

Figure 2.

Chronic hepatitis C patient with biopsy-confirmed cirrhosis. Coronal T2-W (a), axial T2-W (b), axial In (c) and opposed phase (d), post contrast arterial phase (e), portal venous phase (f) and elastogram (h) at the same level, and delayed phase image (g) at an inferior level. R1 graded parenchyma texture-4 (fibrosis definitely present), regenerative nodule-absent, surface nodularity-mild and overall impression-6 (advanced cirrhosis). R2 graded parenchyma texture-3 (fibrosis probably present), regenerative nodule-absent, surface nodularity-absent and overall impression-4 (fibrosis present). Both readers reported collaterals, EGBF, and RPHN negative. Splenomegaly was considered positive. The PPS (8.4mm) was not enlarged. The mean stiffness measured by the MRE readers R3 and R4 were 8.23 and 8.4kPa and both correctly classified the case as positive for cirrhosis.

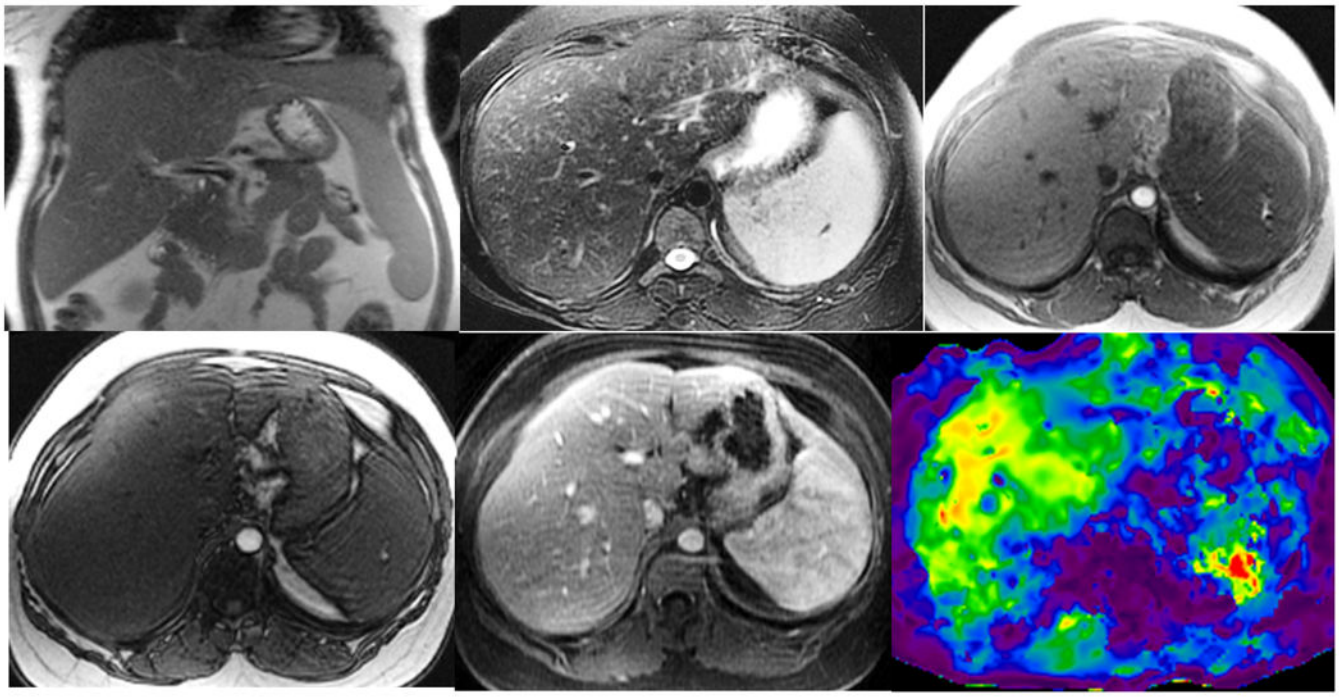

Figure 3.

Non-alcoholic steatohepatitis with biopsy proven stage 1 liver fibrosis. Coronal T2-W (a), axial T2-W (b), axial In-(c) and opposed phase (d), gadolinium enhanced portal venous phase (e), and elastogram (f) at the same level. Note mild splenomegaly. Histology showed mild steatohepatitis of grade 1 of 3 and mild zone 3 fibrosis stage 1 of 4. Her serum liver enzymes level were mildly raised. The overall impression with MRI for two readers R1 and R2 were 3 (mild fibrosis) and 4 (significant fibrosis) respectively. The mean liver stiffness measured by the MRE readers R3 and R4 were 5.1 and 4.4 kPa consistent with significant fibrosis.

Table 1

MRI sequences and parameters

Sequence	Plane	FOV (cm)	Phase FOV	Slice Thickness (mm)	Slice gap (mm)	Matrix	TR/TE (ms)	Flip angle	Bandwidth (kHz)
SSFSE	Coronal	38-44	1.0	5	1	256×224	1600/85	90	82
FSE	Axial	32-44	0.7-1.0	5	1	256×224	/85	90	32
In/Opp	Axial	32-44	0.75	6	1	256×192	115/2.2, 4.4	70	32
LAVA	Axial	36-44	0.8	3.0-3.6		256×224	3.4/1.6	15	82
SPGR	Axial	32-44	0.75	6	1	256×192	130/3.6	70	32
FRFSE	Axial	34-44	0.8	6	1	256×192	2000/85	90	32

SSFSE- single shot fast spin echo;

FSE- fast spin echo, respiratory triggered with TR=2 respiratory intervals, echo train length of 8 to 16

In/Opp- In and opposed phase

LAVA- Liver Acquisition with Volumetric Acceleration (3D SPGR with spectral fat saturation), parallel imaging acceleration factor = 2

SPGR- Spoiled gradient recovery

FRFSE- Fast Recovery Fast Spin Echo, optional sequence used as an alternative to FSE when respiratory triggering was poor. Echo train length of 19

Table 2

Interobserver agreement results for MRI features

MRI feature	Kappa (95% CI)
Parenchyma texture	0.28 (0.17 - 0.40)
Regenerative nodules	0.56 (0.31 - 0.80)
Surface nodularity	0.74 (0.61 - 0.86)
Right posterior hepatic notch (RPHN)	0.45 (0.15 - 0.74)
Expanded gall bladder fossa (EGBF)	0.12 (-0.14 - 0.38)
Ascites	0.75 (0.55 - 0.96)
Splenomegaly	0.75 (0.58 - 0.92)
Varices	0.68 (0.48 - 0.88)
Overall impression	0.55 (0.43 - 0.66)

Table 3

Sensitivity, specificity and accuracy of MRI features and MRE for detection of significant fibrosis

Characteristic	Sensitivity	Specificity	Accuracy
Parenchyma texture	87.9 (71.8-96.6)	55.2 (35.7-73.6)	71.5 (58.6-82.3)
Regenerative nodules	48.5 (30.8-66.5)	96.5 (82.2-99.9)	72.5 (59.7-83.1)
Surface nodularity	60.6 (42.1-77.1)	100 (88.1-100)	80.3 (68.2-89.3)
Overall Impression	66.7 (48.2 - 82.0)	96.5 (82.2 - 99.9)	81.6 (69.7-90.3)
MRE	100 (89.4-100)	96.5 (82.2-99.9)	98.9 (92.1-100)

Table 4
Sensitivity, specificity and accuracy of MRI and MRE for detection of cirrhosis

Characteristic	Sensitivity	Specificity	Accuracy
MRI features			
Parenchyma texture	76.5 (50.1-93.2)	84.4 (70.5-93.5)	80.5 (68.4-89.4)
Regenerative nodules	70.6 (44.0-89.7)	88.9 (75.9-96.3)	79.7 (67.6-88.9)
Surface nodularity	41.2 (18.4-67.1)	95.6 (84.9-99.5)	68.4 (55.3-79.6)
EGBF sign	41.2 (18.4-67.1)	80 (65.4-90.4)	60.6 (47.4-72.8)
RPHN sign	47.1 (23.0-72.2)	86.7 (73.2-94.9)	66.9 (53.8-78.3)
Varices	70.6 (44-89.7)	77.8 (62.9-88.8)	74.2 (61.5-84.5)
Splenomegaly	82.3 (56.6-96.2)	75.6 (60.5-87.1)	79.0 (66.7-88.3)
Ascites	52.9 (27.8-77.0)	86.7 (73.2-94.9)	69.8 (56.8-80.8)
Enlarged PPS	56.2 (29.9-80.2)	78.6 (63.2-89.7)	67.4 (53.8-79.1)
CRL ratio	52.9 (27.8-77.0)	84.4 (70.5-93.5)	68.7 (55.7 -79.9)
mCRL ratio	58.8 (32.9-81.6)	64.4 (48.8-78.1)	61.6 (48.4-73.7)
Overall Impression	70.6 (44.0-89.7)	88.9 (75.9-96.3)	79.7 (67.6-88.9)
MRE	88.2 (63.6-98.5)	91.1 (78.8-97.5)	93.5 (84.2-98.2)

EGBF- Expanded gall bladder fossa; RPHN- Right posterior hepatic notch ; PPS- Periportal space; CRL- caudate to right lobe liver ratio; mCRL- modified caudate to right lobe liver ratio.